A&A 475, 301–308 (2007)
DOI: 10.1051/0004-6361:20077898

Astronomy & Astrophysics

Synthetic NLTE accretion disc spectra for the dwarf nova SS Cygni during an outburst cycle

M. Kromer[1,2], T. Nagel[1], and K. Werner[1]

[1] Institut für Astronomie und Astrophysik, Universität Tübingen, Sand 1, 72076 Tübingen, Germany
e-mail: nagel@astro.uni-tuebingen.de
[2] Max-Planck-Institut für Astrophysik, Karl-Schwarzschild-Straße 1, 85741 Garching, Germany

Received 16 May 2007 / Accepted 14 August 2007

ABSTRACT

Context. Dwarf nova outbursts result from enhanced mass transport through the accretion disc of a cataclysmic variable system.
Aims. We assess the question of whether these outbursts are caused by an enhanced mass transfer from the late-type main sequence star onto the white dwarf (so-called mass transfer instability model, MTI) or by a thermal instability in the accretion disc (disc instability model, DIM).
Methods. We compute non-LTE models and spectra of accretion discs in quiescence and outburst and construct spectral time sequences for discs over a complete outburst cycle. We then compare our spectra to published optical spectroscopy of the dwarf nova SS Cygni. In particular, we investigate the hydrogen and helium line profiles that are turning from emission into absorption during the rise to outburst.
Results. The evolution of the hydrogen and helium line profiles during the rise to outburst and decline clearly favour the disc-instability model. Our spectral model sequences allow us to distinguish inside-out and outside-in moving heating waves in the disc of SS Cygni, which can be related to symmetric and asymmetric outburst light curves, respectively.

Key words. accretion, accretion disks – stars: dwarf novae – stars: binaries: close

1. Introduction

Dwarf novae (DN) belong to the non-magnetic cataclysmic variables which are binary systems consisting of a white dwarf as primary component and an orbiting late-type main sequence star. Due to their close orbit, mass transfer from the secondary onto the primary via Roche lobe overflow occurs. Because of conservation of angular momentum an accretion disc forms around the white dwarf (Warner 1995).

Dwarf novae are characterised by more or less regular outbursts during which the system undergoes a rise in optical brightness of 2−6 mag. The observed outbursts can be divided into two categories, depending whether the lightcurves are symmetric or not. For asymmetric outbursts they are characterised by a fast rise and slower decline and show a delay of the rise in the UV against the optical. For symmetric outbursts UV and optical fluxes rise simultaneously on a longer timescale than the asymmetric outbursts. Sometimes for both types plateaus are observed during maximum. It is commonly accepted that the outbursts are caused by a luminosity increase in the disc that arises from a temporarily increased mass transport through the disc. The origin of this increased mass transport, however, has been discussed controversially.

According to the mass transfer instability model (MTI, Bath 1975) an instability in the secondary star leads to a temporarily increased mass transfer rate $\dot{M}_2$ from the secondary onto the disc, so that also the mass transport through the disc increases. Because the instability originates in the secondary, the outbursts must start at the outer edge of the disc and proceed inwards in the framework of this model.

In the disc instability model (DIM, Osaki 1974) the mass transfer from the secondary is constant and the outbursts are attributed to thermal viscous instabilities in the disc that lead to a temporarily increased mass transport through the disc. Meyer & Meyer-Hofmeister (1981) and Faulkner et al. (1983) have shown that this instability is due to the local ionisation of hydrogen. Radial temperature and viscosity gradients lead to the propagation of heating or cooling waves throughout the disc, which carry the whole disc over to outburst or quiescence, respectively. In particular this allows the outbursts to start any place in the disc so that outbursts can proceed inwards or outwards.

Today the DIM is generally favoured over the MTI. This is due to the existence of a detailed theoretical framework for the DIM that can explain the outburst behaviour and the different outburst types in a natural manner. According to Smak (1984a) the different rise times for asymmetric and symmetric outbursts are caused by different propagation directions of the outbursts: for the asymmetric outbursts (type-A after Smak 1984a) the heating wave originates in the outer part of the disc and proceeds inside moving with the mass stream, so that the heating wave can move relatively fast. Finally the hot inner part of the disc switches to outburst, so that the rise in the UV is delayed against the optical. In contrast to the symmetric type-B outbursts, the heating wave proceeds inside-out and therefore has to move against the mass stream, resulting in a relatively slow rise. In this case the hot inner parts of the disc are the first to switch to outburst so that optical and UV fluxes increase simultaneously.

Furthermore, that no luminosity increase in the hotspot – the region of the disc, where the mass stream from the secondary impinges – is observed during an outburst contradicts the MTI

model, because such a luminosity increase would be expected if the mass transfer from the secondary increases.

A possibility of distinguishing between both models by observational data arises if one is able to decide whether the outbursts proceed outside-in or inside-out. This can be achieved by comparing time-resolved spectra for an entire outburst cycle with the appropriate model spectra because quiescence and outburst spectra differ significantly. In quiescence the optical spectrum shows the strong hydrogen Balmer emission lines characteristic of an optically thin disc. In contrast, during outburst, broad absorption features in the Balmer series indicate an optically thick disc. At the same time, the intensity in the blue wavelength range increases particularly strongly indicating a rise in the disc temperature.

To this end we calculated time-resolved model spectra (Sect. 3) tailored to the dwarf nova SS Cyg. This is the brightest known DN, showing an outburst brightness of $V = 8.2$ mag (Ritter & Kolb 2003), making it one of the best-studied DN. Before presenting these models in Sect. 3, we give a short overview of our approach in Sect. 2. The results are discussed in Sect. 4.

2. Model assumptions

To calculate the accretion disc spectra we use our accretion disc code AcDc (Nagel 2003; Nagel et al. 2004), which is based on the assumption of a geometrically thin disc (total disc thickness H is much smaller than the disc diameter). This allows us to decouple vertical and radial structures and, together with the assumption of axial symmetry, to separate the disc into concentric annuli of plane-parallel geometry. Then radiative transfer becomes a one-dimensional problem.

Each of these disc rings, which are located at a given radial distance r from the white dwarf, is assumed to be stationary. Thus it can be characterised by a constant mass transport rate $\dot{M}$. The rate of energy generation from viscous shear then becomes independent of the kinematic viscosity ν_k and can be parameterised by the effective temperature

$$T_\mathrm{eff}(r) = \left[\frac{3GM_1\dot{M}}{8\pi\sigma r^3}\left(1-\sqrt{\frac{r_1}{r}}\right)\right]^{1/4} \quad (1)$$

(for example Warner 1995). Thereby M_1 denotes the mass, r_1 the radius of the primary white dwarf, G the gravitational constant, and σ the Stefan-Boltzmann constant.

To get a self-consistent solution, the radiative transfer equation, the hydrostatic and energy equilibrium equations, as well as the NLTE rate equations, that determine the occupation numbers of the atomic levels, are solved simultaneously by an iterative scheme. Therefore detailed information about the involved atomic levels is needed, which is provided in the form of a model atom (cf. Rauch & Deetjen 2003). The kinematic viscosity, which is needed for the vertical structure calculation, can be parameterised by the α-approach of Shakura & Sunyaev (1973)

$$\nu_\mathrm{k} = \alpha c_\mathrm{s} H \quad (2)$$

(where c_s is the speed of sound and $\alpha \leq 1$ a dimensionless parameter) or after Lynden-Bell & Pringle (1974) by the Reynolds number Re

$$\nu_\mathrm{k} = \frac{r v_\phi}{Re} = \frac{\sqrt{GM_1 r}}{Re}, \quad (3)$$

where v_ϕ is the Kepler velocity. We choose the latter approach that is numerically easier to implement because we save a further iteration to solve consistently for c_s and H.

Irradiation of the disc by the primary is considered via the upper boundary condition for the radiative transfer equation. For that purpose the irradiation angle β for each disc ring and the spectrum of the primary must be specified. The spectrum of the primary is parameterised by a blackbody temperature T_bb, or detailed white dwarf model atmosphere spectra are calculated.

The complete set of input parameters, which we must provide for each disc ring, thus consists of $M_1, r_1, \dot{M}, r, Re, \beta, T_\mathrm{bb}$. The spectrum of the complete disc is then obtained by integrating the spectra of these disc rings for different inclination angles, the spectral lines are Doppler shifted according to the radial component of the Keplerian rotation velocity in the disc.

As the accretion discs of dwarf novae are fed by a late-type main sequence star, we assume a disc composition of hydrogen and helium with relative solar abundances. The model atoms used for the disc model calculations presented here contain the ionisation stages H I, H II, and He I-He III. The number of NLTE levels and lines considered is 15 and 105 for H I, 29 and 61 for He I, and 14 and 78 for He II. We consider the H^- opacity and Rayleigh scattering for H and He, which is important for the coolest regions of the disc model. In addition, the Ly_α line in the cool models for the quiescent disk is so broad that it contributes considerably to the source function in the optical band. The reason is that most of the hydrogen (about 90−99%) is neutral throughout most of the line-forming region (Fig. 1, second panel from top).

3. Models

In the following we present detailed models for the accretion disc of SS Cyg in outburst and quiescence. SS Cyg is the brightest known DN and belongs to the U Gem type of DN. For our models we have chosen the orbital parameters according to Ritter & Kolb (2003), who give $M_1 = (1.19 \pm 0.02)\ M_\odot$ for the mass of the white dwarf. According to the mass-radius relation, this corresponds to a white dwarf radius of 3.9×10^8 cm. Together with the mass of the companion $M_2 = (0.704 \pm 0.002)\ M_\odot$ and the orbital period $P = 6.6031$ h, the tidal radius – the radius where the disc is disrupted by tidal interactions with the secondary – follows from

$$r_\mathrm{tidal} = 0.60 \cdot \frac{a}{1+q} \quad (4)$$

(Hellier 2001) and amounts to $r_\mathrm{tidal} = 5.78 \times 10^{10}$ cm. Here a denotes the distance between primary and secondary, and it can be calculated from the third Kepler law. q is the mass ratio $\frac{M_2}{M_1}$. The minimal extension of the disc is given by the so-called circularisation radius

$$r_\mathrm{circ} = r_{\mathrm{L}_1}^4 \cdot \frac{1+q}{a^3} \quad (5)$$

at which the angular momentum is equal to the angular momentum at the Lagrange point L_1. The Roche lobe and therefore the distance r_{L_1} of the Lagrange point L_1 must be calculated numerically. After Plavec & Kratochvil (1964), however, for $0.1 < q < 10$ the approximation

$$r_{\mathrm{L}_1} = a \cdot (0.500 - 0.227 \log q) \quad (6)$$

is possible. This finally leads to $r_\mathrm{circ} = 1.65 \times 10^{10}$ cm. In this radial range we have increased the disc's outer edge r_o until the double-peaked line profiles matched the observation, so we chose $r_\mathrm{o} = 4 \times 10^{10}$ cm. A lower value would give line profiles

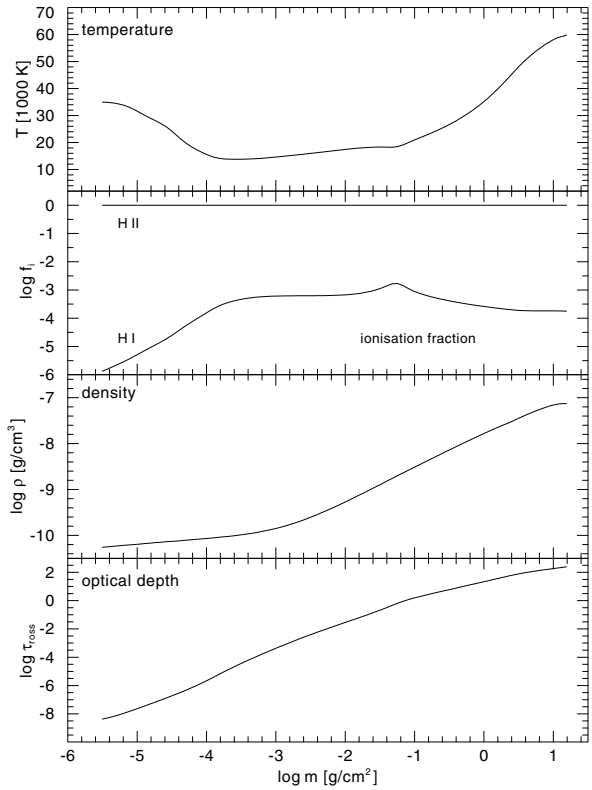

Fig. 1. Vertical structure of the hot disc at a distance of 7.35×10^9 cm from the white dwarf. The physical variables are plotted against the column mass measured from the surface towards the midplane.

that are too broad due to the higher Kepler rotation velocity for smaller radii.

The inner edge of the disc model was fixed from the following arguments. Our model cannot be applied to the boundary layer expected at the transition from the disc to the primary, so we must truncate the disc well before the white dwarf. Despite the higher temperatures in the inner disc, this has little influence on the optical spectrum because the surface area of the inner parts of the disc is much smaller than that of the outer parts. Thus the inner parts can be neglected for modelling optical spectra. In contrast, in the UV range there will be strong imprints from the inner disc portions (cf. Fig. 2).

For the inclination angle i we have chosen 40°, which is consistent with the value of $i = (37 \pm 5)^\circ$ given by Ritter & Kolb (2003). All disc rings have been irradiated with a 50 000 K blackbody spectrum. This temperature is compatible with the observational results for the WD in SS Cyg (Long et al. 2005; Smak 1984b). Tests with a 50 000 K white dwarf model atmosphere have shown that the blackbody approximation has little influence on the emerging disc spectra. The irradiation angle was set to 1°. According to the system geometry, this is possible but probably marks an upper limit. For such small angles, the irradiation increases the effective temperature of the disc ring compared to the value expected according to Eq. (2) only marginally. The relative differences are below 10^{-3} and decrease with increasing r.

3.1. Outburst

For the hot disc during outburst, we assume a constant mass transport rate through the disc of $\dot{M} = 4 \times 10^{-9}\ M_\odot/\mathrm{yr}$ and a constant viscosity of $\alpha \approx 0.30$ according to the DIM. With those parameters, we calculated a disc model from

Table 1. Parameters of the rings for the hot disc in SS Cyg.

#	$r\,[10^9\,\mathrm{cm}]$	Re	T_eff [K]	τ_tot	$h\,[10^8\,\mathrm{cm}]$
1	1.00	3200	74 912	104	0.21
2	1.10	3200	71 056	110	0.23
3	1.22	3000	66 935	114	0.26
4	1.35	2900	63 013	119	0.30
5	1.50	2800	59 074	124	0.34
6	1.66	2600	56 742	125	0.39
7	1.84	2500	51 916	127	0.44
8	2.05	2400	48 403	128	0.50
9	2.30	2350	44 873	130	0.58
10	2.60	2300	41 350	131	0.67
11	2.97	2300	37 798	134	0.79
12	3.43	2300	34 259	139	0.93
13	4.02	2200	30 705	145	1.13
14	4.80	2100	27 135	155	1.40
15	5.85	1700	23 610	163	1.81
16	7.35	1620	20 080	192	2.38
17	9.65	1550	16 525	221	3.29
18	13.50	1450	12 969	258	4.93
19	21.00	1200	9404	169	8.14
20	40.00	500	5862	1.61	16.18

τ_tot is the total Rosseland optical depth from top to disc midplane and $h = H/2$ the vertical extension of the disc from the midplane. The other symbols are defined in the text.

$1 \times 10^9\,\mathrm{cm} \le r \le 4 \times 10^{10}\,\mathrm{cm}$ by dividing the disc into 20 rings to obtain a smooth distribution of $T_\mathrm{eff}(r)$ with a maximal difference of ∼3500 K between neighbouring rings (see Table 1). The resulting disc is optically thick except for the outermost ring. This ring's effective temperature of 5862 K is more typical for a cold disc.

As an example of the vertical structure of the disc model, the temperature, hydrogen ionisation fraction, density, and optical depth are plotted against the height above the disc midplane in Fig. 1 at a distance of 7.35×10^9 cm from the white dwarf. The temperature shows an inversion at the disc surface due to the heating by irradiation of the WD before a strong drop down at $\log m \approx -4$ occurs and then the temperature rises slowly towards the disc's midplane. At $\log m \approx -1$ the disc becomes optically thick.

Figure 2 shows the integrated spectrum of the hot disc and the contribution of selected disc rings. Doppler broadening due to the Keplerian velocity is taken into account. In the optical it is characterised by hydrogen Balmer absorption lines. In the UV, strong absorption lines of the hydrogen Lyman series and He II appear. The latter lines originate in the inner disc rings, where T_eff becomes high enough to populate He II levels. This high T_eff is also the reason the inner disc rings dominate the spectrum in the UV range despite their small surface area compared to the outer rings. The situation is completely different in the optical. There the disc spectrum is dominated by the outermost ring due to its large surface area, so the weak absorption line of He II at 4686 Å, which is visible in the inner ring spectra, is outshone by the much larger continuum flux of the outer rings.

For a comparison to observational results, Fig. 3 shows our synthetic spectrum of the hot accretion disc with the spectra of Clarke et al. (1984), who observed SS Cyg during a rise to outburst.

3.2. Quiescence

Wood et al. (1986) studied the radial temperature distribution in the accretion disc of the DN Z Cha by eclipse mapping. In

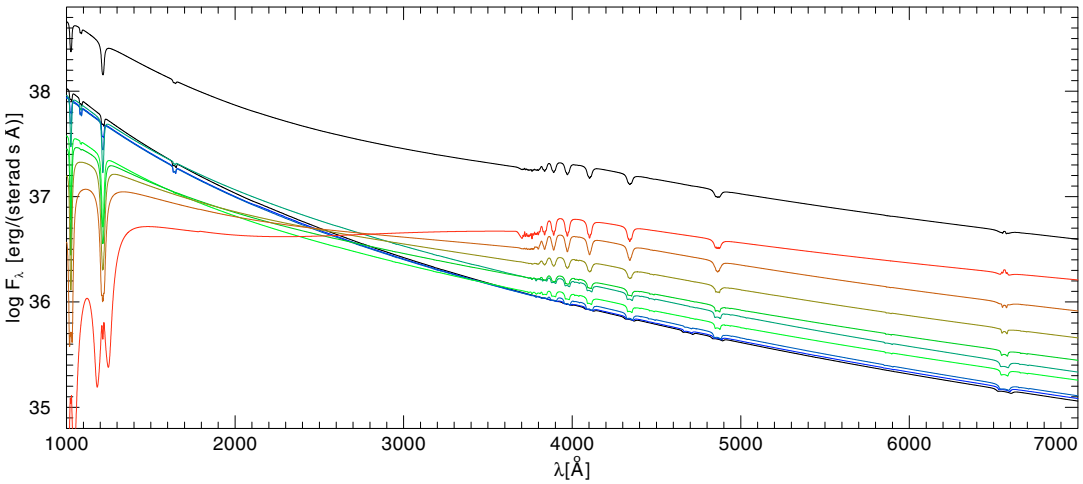

Fig. 2. Model spectra for the accretion disc of SS Cyg in outburst (uppermost curve). The other curves show the contribution of selected individual disc rings starting with the outermost ring (*top*) and then continuing towards the inner disc edge. The inclination angle is 40°.

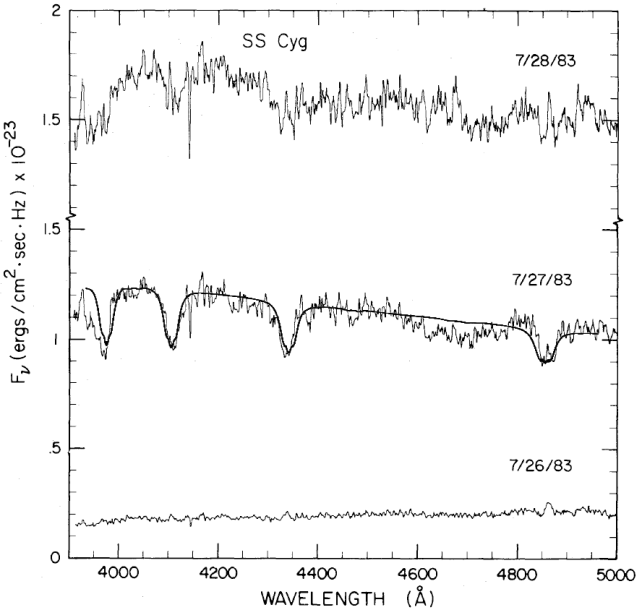

Fig. 3. Observed spectra of SS Cyg (from Clarke et al. 1984) during rise to outburst (outburst maximum corresponds to 7/28/83). Overplotted is our synthetic spectrum for the accretion disc in outburst. The model flux was multiplied by a constant factor to match the observed continuum flux.

contrast to the $T_{\rm eff} \propto r^{-3/4}$ power law expected for stationary accretion discs, they found a more or less constant value of the effective temperature at a level of several thousand Kelvin. This has been interpreted as a hint that the accretion discs of DN in quiescence are not stationary. Therefore we assumed a constant effective temperature of ∼4200 K throughout the disc, which is in the typical range for cold discs. To achieve this temperature for all rings, we adjusted the mass transport rates through the rings (see Table 2). We also adjusted the Reynolds number to get typical values for α in a disc in quiescence according to the DIM. The resulting kinematic viscosity is smaller than in the hot disc by a factor of 10, except for the outermost ring, where the viscosity is as high as for disc rings in outburst. For this disc ring, it was not possible to construct a low-viscosity model with strong emission lines.

Table 2. Parameters for the ring models of the cold disc in SS Cyg.

#	r [10^9 cm]	$\dot{M}$ [$M_\odot$/yr]	Re	$\tau_{\rm tot}$	h [10^8 cm]
1	4.00	1.4×10^{-12}	19 000	0.27	0.71
2	6.00	4.0×10^{-12}	16 000	0.24	1.13
3	8.00	1.0×10^{-11}	13 000	0.28	1.59
4	9.00	1.4×10^{-11}	13 000	0.30	2.00
5	10.00	1.9×10^{-11}	10 000	0.29	2.34
6	20.00	1.4×10^{-10}	3000	0.28	6.00
7	40.00	1.0×10^{-9}	500	0.22	14.56

The number of disc rings required is much smaller than for the hot disc, as the change in spectral properties across the radius is marginal due to the constant temperature. Furthermore we did not extend the cold disc as far in as the hot disc, but truncated the model at $r = 4 \times 10^9$ cm. This is again justified by the constant effective temperature, which prevents a strong contribution of the inner rings to the UV-flux in contrast to the case of the hot disc (see Fig. 4).

The resulting disc spectrum (Fig. 4) is compared to an observed spectrum taken from Martinez-Pais et al. (1994) in Fig. 5. For that purpose the model spectrum has been normalised to the local continuum flux. In principle, the model reproduces the hydrogen Balmer emission lines, but they are not as strong as in the observation. The He I emission lines are not seen in our model spectrum, and the reason may be that they form in the hot spot, which we have not included in our models.

As an example, the vertical structure of the cold disc is shown in Fig. 6 at a radial distance of 4.0×10^{10} cm. In contrast to the hot disc, the temperature does not increase towards the disc midplane but declines monotonically. Towards the disc surface, the irradiation of the WD again causes a temperature inversion. The entire cold disc is optically thin.

3.3. Rise to outburst

To examine the spectral evolution from quiescence to outburst, we combined rings of the cold and hot discs to a sequence of disc models such that this sequence simulates the propagation of the heating wave throughout the disc. In this way we studied the two different cases of outside-in and inside-out moving heating waves to achieve further insight into the processes taking place

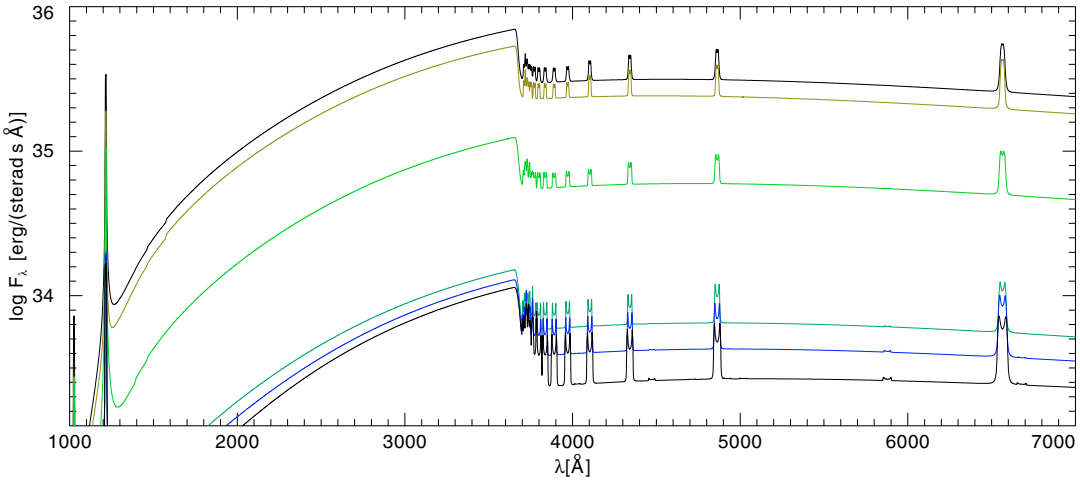

Fig. 4. Model spectra for the accretion disc of SS Cyg in quiescence (uppermost curve). The other curves show the contribution of selected individual disc rings starting with the outermost ring (*top*) and then continuing towards the inner disc edge. The inclination is 40°. The spectral lines are getting broader due to the higher Kepler velocities of the inner disc rings.

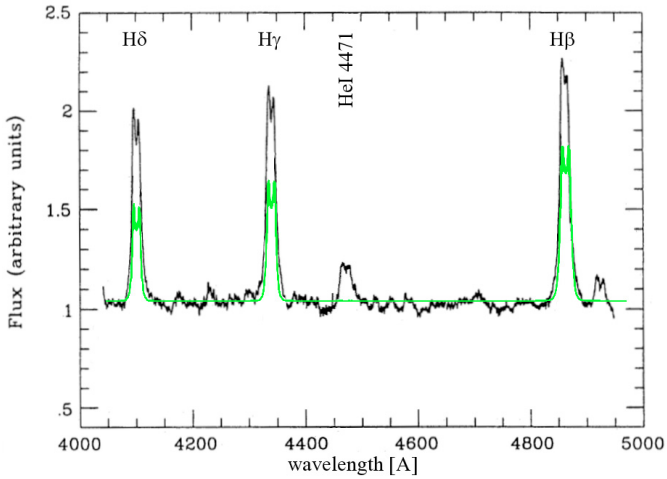

Fig. 5. Observed spectra of the accretion disc of SS Cyg during quiescence (Martinez-Pais et al. 1994). Overplotted is our synthetic spectrum for the accretion disc of SS Cyg in quiescence (grey). The flux was normalised to the local continuum flux.

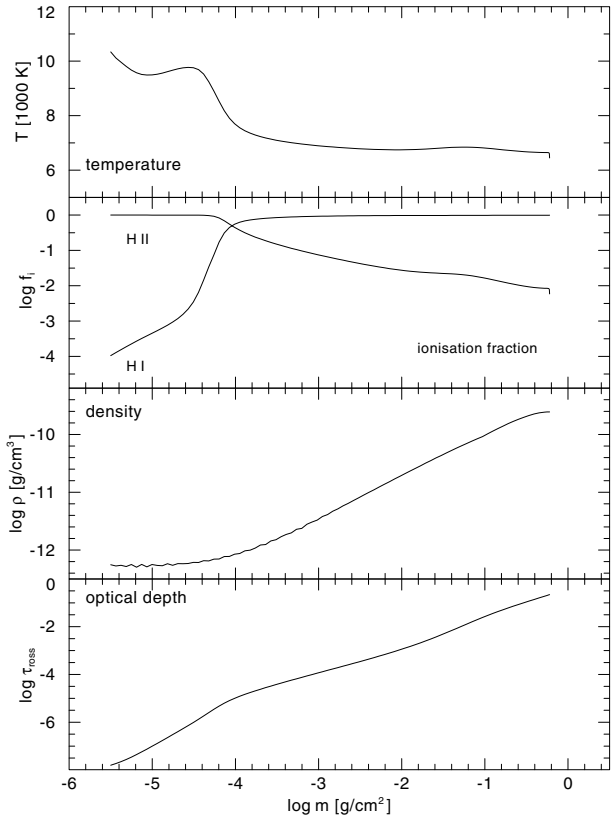

Fig. 6. Vertical structure of the cold disc at a distance of 4.0×10^{10} cm from the white dwarf. The physical variables are plotted against the column mass measured from the surface towards the midplane.

in the disc during rise to outburst. For the outside-in outburst this sequence consists of five disc models in which the cold rings have been replaced by the next-neighbouring hot rings from the outside. The assembly of these models is shown in Table 3.

The left panel of Fig. 7 shows the spectral evolution for this sequence from a pure cold disc to full outburst, as well as the left panel of Fig. 8 where the spectra are normalised to the local continuum. The Balmer series turns from emission to absorption immediately after the outermost disk ring flipped into the hot state, because the overall disc flux in the optical is dominated by the flux of the outer rings and these are dominated by absorption in the hot state.

Similarly we modelled the inside-out outburst by a sequence of five disc models. In the first step the cold disc's innermost ring is replaced by the hot rings that lie inside of its radial position. At the same time the disc is extended inwards to the inner boundary of the hot disc at 1×10^9 cm. For optical spectra, to which we will restrict our discussion in the following, this simplification can be justified because the inner disc rings will only contribute to the UV due to their high effective temperature and because they only cover a small surface area. In the subsequent steps, the next-neighbouring rings from the inside are replaced by hot ones. The complete assembly of the discs for the inside-out model sequence is shown in Table 4.

The right panels of Figs. 7 and 8 show the spectral evolution for this sequence from a pure cold disc to full outburst. In contrast to the outside-in scenario the hydrogen Balmer emission only diminishes slowly during rise to outburst, while increasing absorption wings appear.

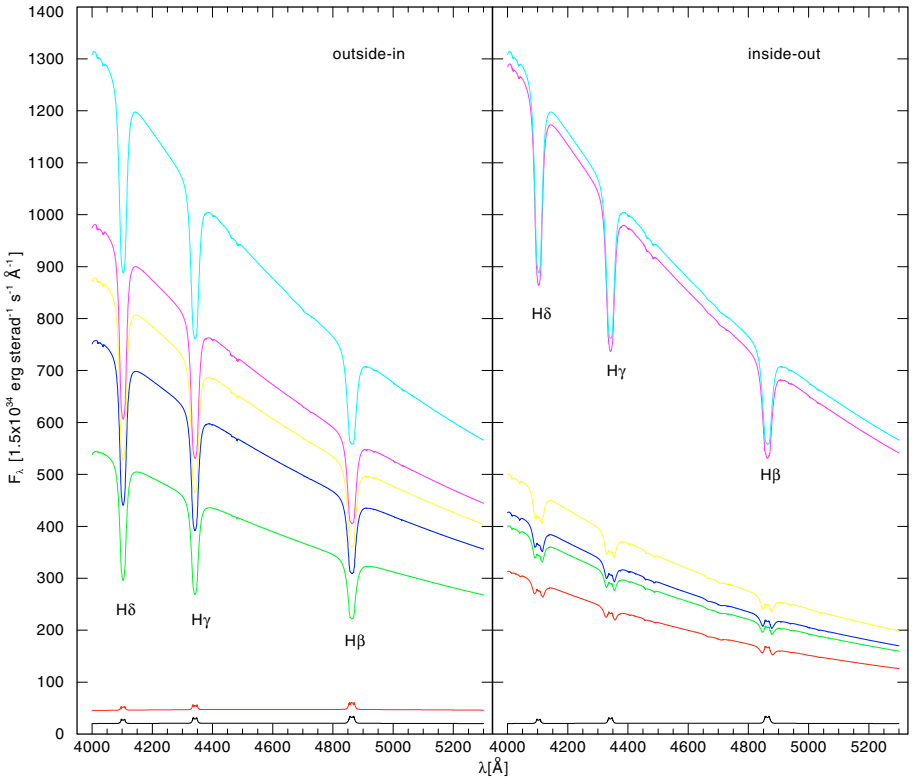

Fig. 7. Spectral evolution between 4000 and 5300 Å for an outside-in outburst (*left panel*) and an inside-out outburst (*right panel*). The lowermost graphs show a pure cold disc that evolves to full outburst (uppermost graph) over steps 1 to 5 of Tables 3 and 4, respectively.

Table 3. Assembly of disc models for the simulated outside-in outburst.

#	Step 1	Step 2	Step 3	Step 4	Step 5
1	4.00cold	4.00cold	4.00cold	4.00cold	4.00cold
2	6.00cold	6.00cold	6.00cold	6.00cold	6.00cold
3	8.00cold	8.00cold	8.00cold	8.00cold	7.35hot
4	9.00cold	9.00cold	9.00cold	9.65hot	9.65hot
5	10.0cold	10.0cold	13.5hot	13.5hot	13.5hot
6	20.0cold	21.0hot	21.0hot	21.0hot	21.0hot
7	40.0hot	40.0hot	40.0hot	40.0hot	40.0hot

Numbers in "step" columns denote the radial position of the model in 10^9 cm, the following "cold" or "hot" label whether a cold or hot ring was used.

One has to keep in mind that the steps of our sequences are not equidistant in time. For an outside-in outburst, for example, the heating wave moves inwards quickly; and according to our models, the spectral lines change from emission to absorption as soon as a part of the outer region is in outburst, so one will observe an absorption-line spectrum during most of the rise of an outside-in outburst. In the case of an inside-out outburst, the heating wave moves rather slowly outwards. As our models show, the line spectrum of the disk does not change to pure absorption until the outermost regions are in outburst. Hence one would observe an emission-line spectrum most of the time of an inside-out outburst.

3.4. Decline

Decline from outburst to quiescence is mediated by a cooling wave. This wave always propagates outside-in as argued by e.g. Warner (1995), so that the cooling can be studied by examining the inside-out moving heating wave of Table 4 in reverse order. According to the right panel of Fig. 7, the hydrogen Balmer lines evolve smoothly from absorption to pure emission.

4. Results and discussion

We used the models presented above to determine the nature of the outbursts in SS Cyg by comparing them to spectra available in the literature. This turned out to be rather difficult, because adequate time-resolved spectra during rise to outburst are very rare even for the well-studied case of SS Cyg.

Martinez-Pais et al. (1996) presented time-resolved spectra for different outbursts of SS Cyg. Among them are two spectra taken during a rise to an outburst of the symmetric type. According to their Fig. 2 the hydrogen Balmer emission lines decrease slowly between these two spectra, while the absorption wings increase like in the right panel of our Fig. 7 for the inside-out outburst. This leads to an identification of symmetric outbursts in SS Cyg with inside-out outbursts, which is in good agreement to Smak's (1984a) description of type-B outbursts, but contrasts to the original conclusion of Martinez-Pais et al. (1996). They interpret the late appearance of the He II 4686 Å line as a consequence of an outside-in propagating heating wave, because they assumed that the He II 4686 Å line originates in the hot inner part of the disc. This is questionable in light of our models. The line should be significantly broader due to the higher Kepler velocity if this assumption is true.

"Some indication of an increase in the hot spot's vertical size and, perhaps, brightness" leads them to conclude further that symmetric outbursts are connected with an instability of the secondary star, so they favoured the MTI for this outburst. This is put into question by our models, which indicate an inside-out outburst in favour of the DIM.

The observations of Clarke et al. (1984) cover a complete outburst cycle of SS Cyg. The outburst shows an asymmetric light curve. Three of its spectra before and during rise, as well as during maximum, are shown in Fig. 3. The spectral evolution of this outburst differs significantly from what was observed by Martinez-Pais et al. (1996): quiescent Balmer line emission abruptly disappears at the onset of rise to maximum, before full

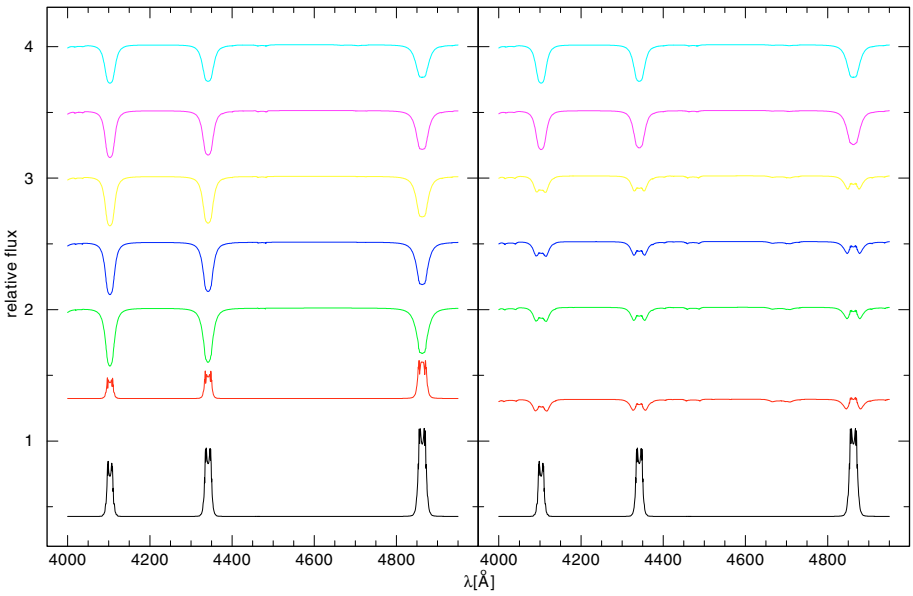

Fig. 8. Spectral evolution between 4000 and 5300 Å for an outside-in outburst (*left panel*) and an inside-out outburst (*right panel*). The spectra are normalised to the local continuum. The lowermost graphs show a pure cold disc that evolves to full outburst (uppermost graph) over steps 1 to 5 of Tables 3 and 4, respectively.

Table 4. Assembly of disc models for the simulated inside-out outburst.

#	Step 1	Step 2	Step 3	Step 4	Step 5
1	1.00hot	1.00hot	1.00hot	1.00hot	1.00hot
2	1.10hot	1.10hot	1.10hot	1.10hot	1.10hot
3	1.22hot	1.22hot	1.22hot	1.22hot	1.22hot
4	1.35hot	1.35hot	1.35hot	1.35hot	1.35hot
5	1.50hot	1.50hot	1.50hot	1.50hot	1.50hot
6	1.66hot	1.66hot	1.66hot	1.66hot	1.66hot
7	1.84hot	1.84hot	1.84hot	1.84hot	1.84hot
8	2.05hot	2.05hot	2.05hot	2.05hot	2.05hot
9	2.30hot	2.30hot	2.30hot	2.30hot	2.30hot
10	2.60hot	2.60hot	2.60hot	2.60hot	2.60hot
11	2.97hot	2.97hot	2.97hot	2.97hot	2.97hot
12	3.43hot	3.43hot	3.43hot	3.43hot	3.43hot
13	4.02hot	4.02hot	4.02hot	4.02hot	4.02hot
14	4.80hot	4.80hot	4.80hot	4.80hot	4.80hot
15	5.85hot	5.85hot	5.85hot	5.85hot	5.85hot
16	6.00cold	7.35hot	7.35hot	7.35hot	7.35hot
17	8.00cold	8.00cold	9.00cold	9.65hot	9.65hot
18	9.00cold	9.00cold	10.0cold	10.0cold	13.5hot
19	10.0cold	10.0cold	20.0cold	20.0cold	21.0hot
20	20.0cold	20.0cold	40.0cold	40.0cold	40.0cold
21	40.0cold	40.0cold	–	–	–

absorption sets in during the rise. This fits our outside-in model sequence, indicating that the asymmetric outbursts are indeed connected to outside-in, i.e. type-A outbursts following Smak (1984a).

The fact that the observed spectra of Clarke et al. (1984) during full maximum do not show pure absorption lines like our model might be a consequence of the radial extension of the disc during outburst. This is not considered in our model, although it is expected in the DIM due to the higher transport of angular momentum during outburst. It might be possible that this portion of the disc outshines the basic inner part of the disc due to its large surface area. If this portion of the disc then has comparable properties to the current outermost grid point, which is relatively cool and emission-dominated, or at least continuum-dominated, the resulting model spectrum of the extended disc might show no absorption lines anymore.

For decline from outburst to quiescence, another study by Hessman et al. (1984) exists. Their Fig. 5 is in good agreement with the right panel of our Fig. 7 if read from top to bottom, which means that they witnessed an outside-in propagating cooling wave. This again agrees with the DIM.

During decline the 4686 Å line of He II often shows a prominent emission feature like in the study of Hessman et al. (1984). This does not appear in our model. If it originates in the disc, it must arise from the inner parts, because only there does $T_{\rm eff}$ become high enough to populate He II levels. Accordingly, the inner rings of our hot disc model show He II 4686 Å, however, not in emission but in absorption. This supports the results of Unda-Sanzana et al. (2006), which identified the gas stream/disc impact region as the origin of the He II 4686 Å emission by means of Doppler tomography.

That Hessman et al. (1984) observed central emission peaks in the Balmer lines right from the beginning of the decline might be indicating that not the complete disc but only the inner parts participated in the outburst. If for example the disc stays cold for $r > 10 \times 10^{10}$ cm, we only have to compare the lower five curves of the right panel in Fig. 7 to the observation. As Hessman et al. (1984) observed a short outburst without plateau, this would be again in good agreement with the DIM. There the short outbursts are attributed to discs that are not completely in outburst, while plateaus are supposed to appear if matter is accreted with a constant rate through a disc that is completely in outburst.

It will be interesting to extend our study to the UV range where especially the C IV 1550 Å line shows a similar behaviour to the Balmer lines. For that purpose, heavier elements must be included in the model calculations, and the influence of the disc wind, which becomes obvious in the P Cyg shaped profile of the C IV 1550 Å line in outburst, will be considered.

Another question is the influence of metal opacities, which we have neglected here, on the hydrogen and helium lines. From our experience in working on stellar atmospheres (O and sdO stars), we would predict that metal line blanketing and surface cooling will produce slightly deeper H and He absorption lines in the hot disk; however, we expect no qualitative change in the optical spectrum. The situation is different in the cool ring models, which are optically thin. Work is in progress to investigate the metal line blanketing problem.

5. Summary

In this paper, we have presented NLTE model calculations for the accretion disc of SS Cyg in outburst and quiescence. The resulting synthetic spectra describe the observed optical spectra and their transition well from absorption during outburst to emission during quiescence.

Simulations of the spectral evolution for outside-in and inside-out propagating heating waves were carried out. We compared them to published observations and conclude that symmetric outbursts belong to the inside-out type. This confirms DIM expectations (e.g. Smak 1984a), which are based on rise-time arguments and explicitly excludes the MTI model. In contrast, asymmetric outbursts seem to be outside-in outbursts.

References

Bath, G. T. 1975, MNRAS, 171, 311
Clarke, J. T., Bowyer, S., & Capel, D. 1984, ApJ, 287, 845
Faulkner, J., Lin, D. N. C., & Papaloizou, J. 1983, MNRAS, 205, 359
Hellier, C. 2001, Cataclysmic Variable Stars (Springer Praxis)
Hessman, F. V., Robinson, E. L., Nather, R. E., & Zhang, E.-H. 1984, ApJ, 286, 747
Long, K. S., Froning, C. S., Knigge, C., et al. 2005, ApJ, 630, 511
Lynden-Bell, D., & Pringle, J. E. 1974, MNRAS, 168, 603
Martinez-Pais, I. G., Giovannelli, F., Rossi, C., & Gaudenzi, S. 1994, A&A, 291, 455
Martinez-Pais, I. G., Giovannelli, F., Rossi, C., & Gaudenzi, S. 1996, A&A, 308, 833
Meyer, F., & Meyer-Hofmeister, E. 1981, A&A, 104, L10
Nagel, T. 2003, Ph.D. Thesis, Eberhard-Karls-Universität Tübingen
Nagel, T., Dreizler, S., Rauch, T., & Werner, K. 2004, A&A, 428, 109
Osaki, Y. 1974, PASJ, 26, 429
Plavec, M., & Kratochvil, P. 1964, Bull. Astr. Inst. Czechosl., 15, 165
Rauch, T., & Deetjen, J. L. 2003, in Stellar Atmosphere Modelling, ed. I. Hubeny, D. Mihalas, & K. Werner, ASP Conf. Ser., 288, 103
Ritter, H., & Kolb, U. 2003, A&A, 404, 301
Shakura, N. I., & Sunyaev, R. A. 1973, A&A, 24, 337
Smak, J. 1984a, PASP, 96, 5
Smak, J. 1984b, Acta Astron., 34, 317
Unda-Sanzana, E., Marsh, T. R., & Morales-Rueda, L. 2006, MNRAS, 369, 805
Warner, B. 1995, Cataclysmic Variable Stars (Cambridge University Press), Cambridge Astrophys. Ser., Cambridge, New York
Wood, J., Horne, K., Berriman, G., et al. 1986, MNRAS, 219, 629